DETERMINATION OF PERFORMANCE CURVES WITH THE BASIC RESULTS AND EXPANDED UNCERTAINTY CRITERIA: A CASE STUDY OF A RAPID CENTRIFUGAL PUMP WITH SINGLE CURVATURE BLADES

Jair Nascimento Filho, Manuel Losada y Gonzalez, Carlos Barreira Martinez
Laboratório de Eficiência Energética e Hibráulica em Saneamento (LENHS) / Centro de Pesquisas Hidráulicas e Recursos Hídricos (CPH) / Universidade Federal de Minas Gerais (UFMG), Av. Antônio Carlos 6627, 31.270-901, Campus Pampulha - Belo Horizonte, MG, Brasil, (jair@demec.ufmg.br, manuel@cpdee.ufmg.br, martinez@cce.ufmg.br)

ABSTRACT

Determination of the performance curves in base form and expanded uncertainty: case study of a rapid centrifugal pump with single curvature blades.

The measurement and determination of variables relating to performance of hydraulic machines are of great importance in the analysis of technical and economic feasibility of hydraulic systems. To obtain a reliable determination of these variables, the research team LENHS UFMG (Laboratory for Energy Efficiency in Hydraulics from the Federal University of Minas Gerais) developed a methodology, based on concepts of metrology. This paper deals with this reliable determination of performance-related motor pump sets variables in the form of basic income and expanded uncertainty.

A case study is presented with a rapid centrifugal pump (specific speed of 160 rpm), endowed with straight cylindrical blades. The above methodology was applied to perform a reliable determination of the performance. The pump was designed, manufactured and tested in the CPH (Hydraulic Research Center).

1 INTRODUCTION

Water and electric power are called essential goods for the life and the society (Water law No. 9.433/1997, 1997, Oliveira, 2010). The hydraulic energy is a type of energy that has water as raw material and, one of its most used applications is the electricity generation.

Water is a renewable good, but it is limited (Almeida e Hernandez, 2001) and, therefore, it is necessary to save and rationally to use it. The optimization of the water distribution networks drawing (Mora et al, 2012; Salcedo et al, 2013) and the operation of systems equipped with a set of motor pumps and frequency inverters (Makino et al, 2012; Camboim et al, 2012) are actions developed and implemented with this purpose. However, whatever the solution adopted for improving the hydraulic systems, the wrong determination of variables such as the flow and efficiency may make unfeasible ventures or cause great damages.

The determination of variables as base result and uncertainty allows that the whole range where the result can happen is known. Valentim (2008) presents pump efficiency results with the aid of determinations of efficiency measurement uncertainties; Nascimento Filho et al (2009) performed the characterization, supported by metrology concepts, of a didactic bench of turbo machines tests;

Nascimento Filho et al (2011) presents a methodology of instrumentation diagnosis used in flow and efficiency measurements.

One of the research lines of LENHS / UFMG is to develop methodologies based on metrology concepts, related to the efficient use of water and electric power. The aim of this work is to show the reliable determination of hydraulic variables related to the performance of a fast centrifugal pump with single curvature blades.

The pump, called UFMG / CPH Pump, was designed and manufactured in a research project with the aim of making available equipment for supplying small charges, typical of developing communities. It is a small-sized pump (3 hp) of specific speed (n_s = 160 rpm) proper for operation with flow versus manometric height ratio superior to the ones from slow pumps. Although the drawing of pumps with rotors with double curvature blades is indicated to specific speeds up to 90 rpm (Macintyre, 1997), the UFMG CPH pump was designed with single curvature blades. This aspect meets the objective of developing a type of equipment which can be easily manufactured in a regular workshop.

2 FAST CENTRIFUGAL PUMP OF SINGLE CURVE BLADES

From a demand of flow and manometric height, a fast centrifugal pump was designed, manufactured and assembled. The design was developed with the aid of a set of traditional equations known in the literature (Andrade, 1967, Macintyre, 1997).

The turbo-pump rotors calculation is generally made from the flow entrance, manometric height and rotation data (Andrade, 1967; Macintyre, 1997). Additionally to these data, in certain situations, the constructive characteristics entering in the process as project conditioning shall be taken into account. In these situations, an adaptation of the customarily used method can be made (Nascimento et al, 2012).

By the Macintyre method (1997), the meridian speeds can be calculated with the aid of built tables based on the rotation. In the situation, the meridian speeds are determined based on the constructive data, with rotors diameters and blades width (Nascimento et al, 2012). The determination of the speeds triangles at the input and output of the channel between blades implies on the definition of the rotor's geometric data. Thus, the procedure for the rotor's calculation is performed through the definition of speeds triangles. It is about a test method based on the speeds determination, for avoiding excessive speeds (Nascimento et al, 2012).

In order to manufacture the pump's casing, a bipartite solution was chosen because it is easier to access the internal part of the same. Thus, it was possible to eliminate occasional superficial imperfections as well as finishing the inlet rings. Notwithstanding these facilities, the bipartite format has the disadvantage of making difficult to manufacture the inlet flange. The bearing blocks are made with ball bearings and they are housed in an aluminum case screwed at the casing diametrically opposed to the pump' suction tube. The use of screws makes easier the set assembly and it allows faster maintenance operations. The motor is coupled to the pump through a flexible joint.

For manufacturing the pump's casing, a template of the volute in wood and epoxy which was later casted in aluminum was manufactured. Figure 1a shows the geometry and dimensions of the pump's volute. Figure 1b shows a view of the casted casing. Figure 2a presents a plain view of steel disks and plates which will be folded for forming the blades. Figure 2b shows a view of the lower plate.

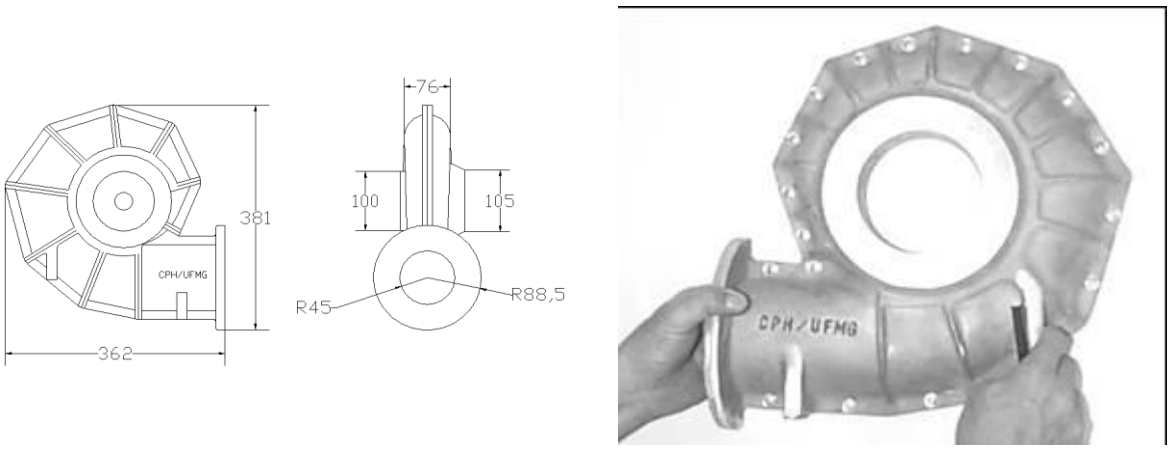

a) b)

Figure 1 – a) Dimensions in mm of the template manufactured; b) View of the volute box casted in aluminum (Source: SEREA 2012, Nascimento et al.)

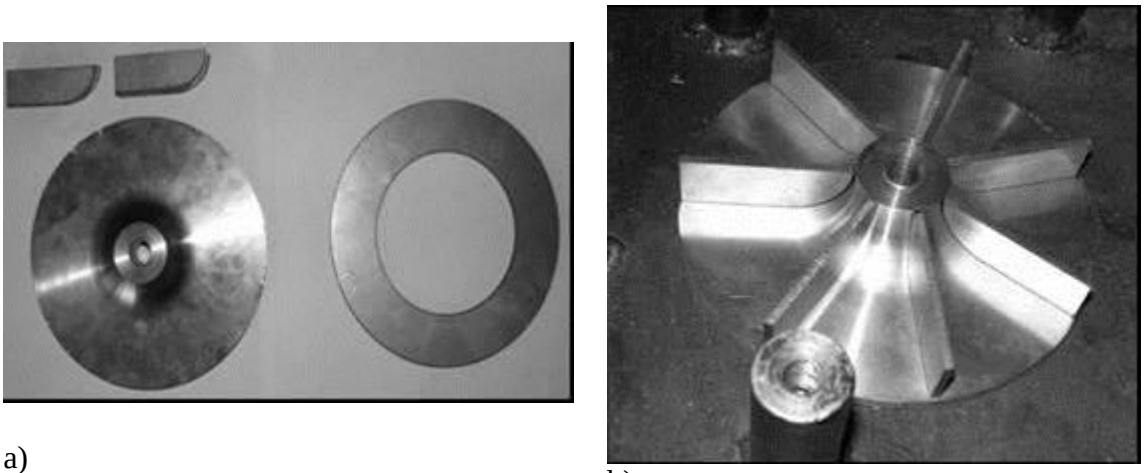

a) b)

Figure 2 – a) View of the rotor's lower and upper disks; b) View of the rotor's lower disk of the pump with the blades positioned (Source SEREA 2012, Nascimento et al.)

The pump's blades were manufactured by the folding (hits in the hot metal) of metal plates later welded to the rotor's disk. The rotor's lower and upper disks were manufactured in carbon steel. After folding the plates, the welding of the same in the upper and lower disks was made. It was chosen to make the full folding (all over the extension) of the blade in the lower disk since the same is heavier. However, the upper disk (ring) was fixed at the blades only in extreme points. This made easier the welding process once one of the faces would inevitably be welded in a very narrow space.

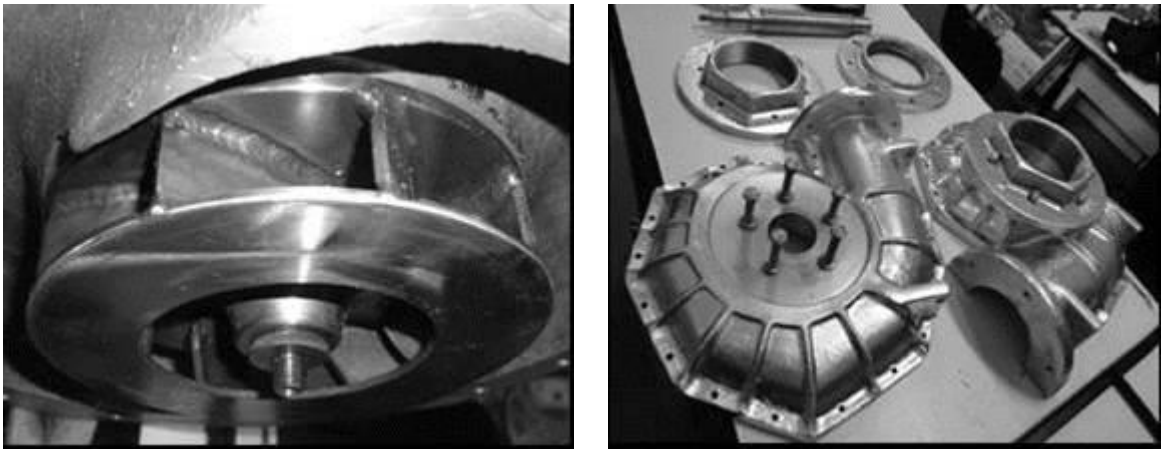

a) b)

Figure 3 – a) View of blades welding details at the rotor's lower disk. 3 b) Casing and suction and output flanges (Source SEREA 2012, Nascimento et al)

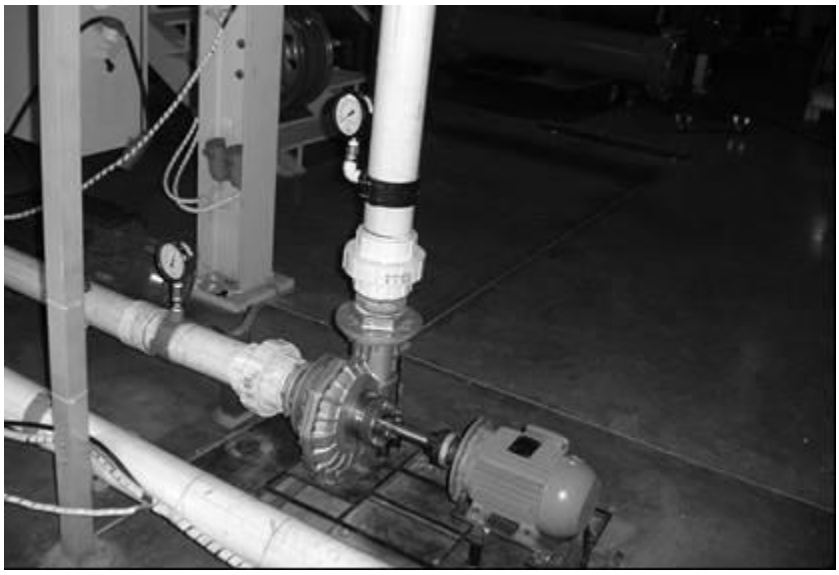

Figure 4 – Photo of the motor pump set assembled at the LENHS UFMG's tests circuit

Figure 3a shows details of the blades welding at the disk. Figure 3b shows the details of the casing's set (two parts) and the suction and output flanges already prepared and connected to the casing through screws. The five couple screws of the bearing block case can be observed. Figure 4 is a photo of the motor pump set assembled at the tests facility.

3 TEST FACILITY

For testing the pump, the assembly of the same is made in a test bench shown in Figures 5 and 6. The essay's facility is built in a 100 mm nominal diameter PVC piping, a lower tank of 3.5 m^3 capacity and an upper tank with 1.5 m^3 capacity.

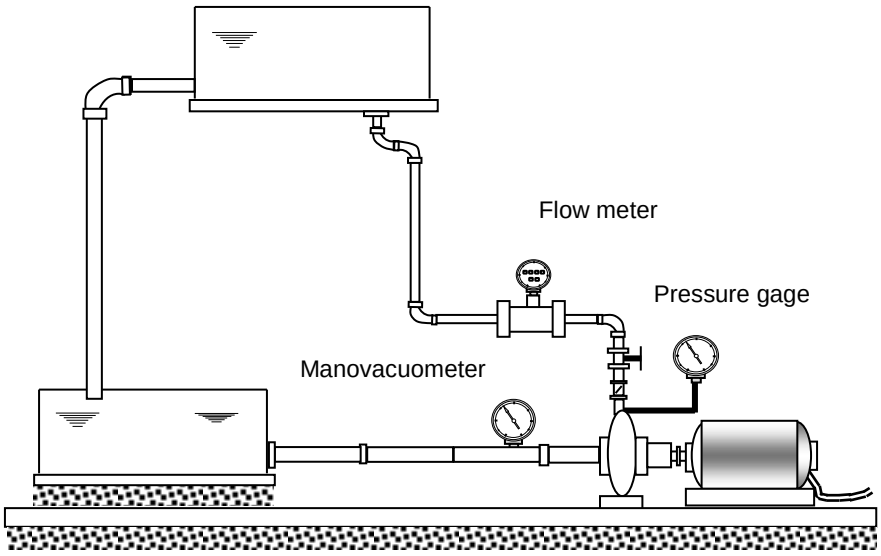

Figure 5 – Motor pump set assembled at the lift facilities of LENHS UFMG

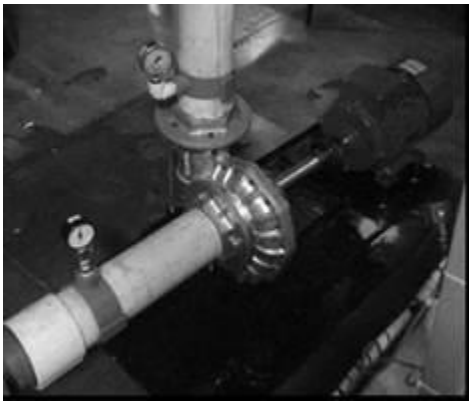

Figure 6 – Another view of the pump

The instrumentation comprises the following measuring devices:

- Endress + Hauser promag F33F electromagnetic flowmeter, nominal diameter of 100mm, measurement error in % of the measure around 0.6% of the indicated value;
- Class B manovacuometer, -1+1 kgf/cm^2 scale or bar, numbering -0.2 / +0.2, subdivision – 0.02/ +0.02, nominal diameter 96 mm, glycerin filling liquid, Famabras brand;
- Class B pressure gage, -0 / 2,5 kgf/cm^2 scale or bar, numbering 0.5 subdivision 0.02, nominal diameter 100 mm, glycerin filling liquid, Famabras brand;
- Electric equipment.

4 TESTS

The test was performed with 8 points of operation, 10 measures in each point. At Table 1, the data collection concerning point 4 and conversion to the SI are presented.

Table 1: Data collection concerning the operation point No. 4 and conversion to the SI.

Hourly [h:min]	p_e [kgf/cm^2]	p_s [kgf/cm^2]	Q [m^3/h]	P_{el} [W]	p_e [kPa]	p_s [kPa]	Qx10^3 [m^3/s]
15:45	0,06	0,90	20,98	2081,3	5,9	88,3	5,828
15:47	0,06	0,90	20,78	2086,4	5,9	88,3	5,772
15:49	0,06	0,90	20,58	2084,1	5,9	87,3	5,717
15:51	0,06	0,89	20,91	2074,5	5,9	88,3	5,808
15:53	0,06	0,90	20,55	2090,5	5,9	87,3	5,708
15:55	0,06	0,89	20,74	2090,5	5,9	88,3	5,761
15:57	0,06	0,90	20,94	2078,2	5,9	88,3	5,817
15:59	0,06	0,90	20,74	2075,7	5,9	88,3	5,761
16:01	0,06	0,90	20,79	2078,5	5,9	88,3	5,775
16:03	0,06	0,90	20,83	2079,3	5,9	88,3	5,786

5 METHODOLOGY

The determination of variables obtained by indirect measurement can be made with the aid of the Equations (1) and (2), where u(x) is the combined uncertainty, $k_{95\%}$, is the Student's coefficient, and $U_{95\%}$ expanded uncertainty with level of trust around 95%.

$$x = \bar{x} \pm U_{95\%}(x) \tag{1}$$

$$U_{95\%}(x) = k_{95\%} u(x) \tag{2}$$

Variables such as η_g, η_b, P, and H, are obtained with the aid of the Equations (3), (4) and (5), where η_g is the global efficiency, η_b is the pump efficiency, P is the water power, P_{axis} is the axis power, P_{el} is the electric power, H is the manometric height, p_e is the pressure at the pump's input, p_s is the output pressure, m is the quota difference between the pressure gages' centers, γ is the specific weight and η_{el} is the electric motor's efficiency.

$$\eta_g = \frac{P}{P_{el}} \tag{3}$$

$$P = \gamma Q H \tag{4}$$

$$H = \frac{p_s \pm p_e}{\gamma} + m \tag{5}$$

$$\eta_{el} = \frac{P_{\text{axis}}}{P_{el}} \tag{6}$$

$$\eta_b = \frac{P}{P_{axis}} = \frac{\eta_g}{\eta_{el}} \tag{7}$$

Using collected data and with the Equations (1) to (7), η_b, H and P_{axis} are obtained as base result and expanded uncertainty for the considered operation point (Eqs. 8a, 8b and 8c).

$$\eta_b = \frac{\overline{Q}}{\overline{\eta}_{el}\overline{P}_{el}}\left[\left(p_s \pm p_e\right) + \overline{m}\,\overline{\gamma}\right] \pm k_{95\%} u(\eta_b) \tag{8a}$$

$$H = \left[\frac{\left(p_s \pm p_e\right)_{med}}{\overline{\gamma}} + \overline{m}\right] \pm k_{95\%} u(H) \tag{8b}$$

$$P_{axis} = \overline{\eta}_{el}\overline{P}_{el} \pm k_{95\%} u(P_{axis}) \tag{8c}$$

The combined uncertainties $u(\eta_b)$ and $u(H)$ are determined according to ISO-GUM (ABNT, 1998).

$$u^2(\eta_b) = \left(u^*(p_e)\right)^2 + \left(u^*(p_s)\right)^2 + \left(u^*(m)\right)^2 + \left(u^*(\gamma)\right)^2 + \left(u^*(Q)\right)^2 + \left(u^*(P_{el})\right)^2 + \left(u^*(\eta_{el})\right) \quad (9a)$$

$$u^2(\eta_b) = \left(\frac{\overline{Q}}{\overline{\eta}_{el}\overline{P}_{el}}u(p_e)\right)^2 + \left(\frac{\overline{Q}}{\overline{\eta}_{el}\overline{P}_{el}}u(p_s)\right)^2 + \left(\frac{\overline{\gamma}\overline{Q}}{\overline{P}_{el}}u(m)\right)^2 + \left(\frac{\overline{m}\overline{Q}}{\overline{\eta}_{el}\overline{P}_{el}}u(\gamma)\right)^2 + \left(\frac{\overline{\eta}_b}{\overline{Q}}u(Q)\right)^2 + \left(\frac{\overline{\eta}_b}{\overline{P}_{el}}u(P_{el})\right)^2 + \left(\frac{\overline{\eta}_b}{\overline{\eta}_{el}}u(\eta_{el})\right)^2 \quad (9b)$$

$$u^2(H) = \left(u^+(p_e)\right)^2 + \left(u^+(p_s)\right)^2 + \left(u^+(m)\right)^2 + \left(u^+(\gamma)\right)^2 \quad (10a)$$

$$u^2(H) = \left(\frac{1}{\overline{\gamma}}u(p_e)\right)^2 + \left(\frac{1}{\overline{\gamma}}u(p_s)\right)^2 + \left(u(m)\right)^2 + \left(\frac{(p_s \pm p_e)_{med}}{(\overline{\gamma})^2}u(\gamma)\right)^2 \quad (10b)$$

$$u^2(P_{axis}) = \left(u^x(p_{el})\right)^2 + \left(u^x(\eta_{el})\right)^2 \quad (11a)$$

$$u^2(P_{axis}) = \left(\eta_{el}u(p_{el})\right)^2 + \left(P_{el}(\eta_{el})\right)^2 \quad (11b)$$

For establishing the standard uncertainties of p_e, p_s, P_{el}, γ, m, and Q, it is necessary taking into account the characteristics of the measurement instruments and the flow variability (equation (12)).

$$u(x) = \sqrt{u(x)^2_{meter} + u(x)^2_{\text{process}}} \quad (12)$$

The uncertainty $u(x)_{meter}$ (rectangular distribution is considered), related to the physical characteristics of the measurement instrument and, the uncertainty $u(x)_{process}$ related to the variability of the phenomenon are obtained with the aid of the Eqs. (13) and (14) respectively, taking n indications in each point of the operation.

$$u(x)_{meter} = \frac{E_{máx}(x)}{\sqrt{3}} \quad (13)$$

$$u(x)_{\text{process}} = \sqrt{\frac{\sum_{i=1}^{n}\left(x_i - \bar{x}\right)^2}{n-1}} \quad (14)$$

As a numeric example, point 4 (Table 2) is taken. For p_s there is Emax of 0.02 kgf/cm^2, in other words 1.96 kPa. With the aid of (12), (13) and (14) there is:

$$u(p_s)_{meter} = \frac{E_{máx(p_s)}}{\sqrt{3}} = \frac{1{,}96\,kPa}{\sqrt{3}} = 1{,}13\,kPa$$

$$u(p_s)_{process} = s(p_s) = \sqrt{\frac{\sum_{i=1}^{n}(p_{si} - \overline{p}_s)^2}{n-1}} = \sqrt{\frac{\sum_{i=1}^{10}(p_{si} - \overline{p}_s)^2}{9}} = 0{,}41kPa$$

Similarly, there is $u(p_e)$, $u(P_{el})$, $u(m)$ and, (refer to Table 2). It is observed that the quota measurement between pressure gages does not depend on process, only on constructive data, therefore $u_{process}\ (m)$ is null. It is observed that the ratio $E_{máx(Q)}/Q$ is 0.006 (provided by the manufacturer) and, taking into account the rectangular distribution for the calculation of $u(Q)_{meter}$, there is (refer to Table 2):

$$u(Q)_{meter} = \frac{u(Q)}{Q}\overline{Q} = \frac{1}{\sqrt{3}}\frac{Emáx(Q)}{Q}\overline{Q} \tag{15}$$

For establishing $u(\gamma)_{process}$, it was considered the temperature variation in the fluid from 15 °C to 30 °C. The specific volume obtained from thermodynamic properties tables is 0.001000 m^3/kg for 15 °C and 0.001004 m^3/kg for 30 °C, which cause specific weight of 9800.19 N/m^3 for 15 °C and 9770.86 N/m^3 for 30 °C. The maximum error was considered as the difference between the average value and the limit values of the considered range. The specific weight is 9785.52 N/m^3, which causes maximum error of 14.66 N/m^3 (refer to Table 2). Errors at the table are insignificant regarding the great temperature range adopted (pessimist enough) and, therefore $u(\gamma)_{meter}$, in other words, $u(\gamma)_{table}$ is considered null (refer to Table 2).

Table 2: Data treatment concerning the operation point nº 4. The m and p indexes mean measuring device and process, respectively.

p_e[kPa]	p_s[kPa]	Qx10^3[m^3/s]	P_{el}[W]			
5,9	88,3	5,828	2081,3			
5,9	88,3	5,772	2086,4			
5,9	88,3	5,717	2084,1			
5,9	87,3	5,808	2074,5			
5,9	88,3	5,708	2090,5			
5,9	87,3	5,761	2090,5			
5,9	88,3	5,817	2078,2			
5,9	88,3	5,761	2075,7			
5,9	88,3	5,775	2078,5			
5,9	88,3	5,786	2079,3			
$p_e$med[kPa]	$p_s$med[kPa]	Qmed[m^3/s]	P_{el}med[W]	m med[m]	γmed[N/m^3]	η_{el}
5,88	88,06	0,005773	2081,9	0,315	9785,52	0,236
$E_{máx}$ [kPa]	$E_{máx}$ [kPa]	$E_{máx}$ [%]	$E_{máx}$ [%]	$E_{máx}$ [m]	$E_{máx}$[N/m^3]	Emáx
1,96	1,96	0,6	0,20	0,003	14,66	0,02
$u(p_e)_m$ [kPa]	$u(p_s)_m$ [kPa]	$u(Q)_m$[m^3/s]	$u(P_{el})_m$[W]	$u(m)_m$[m]	$u(\gamma)_m$[N/m^3]	$u(\eta_{el})_m$
1,13	1,13	0,00002	11,5	0,002	0,0	0,012
$u(p_e)_p$[kPa]	$u(p_s)_p$[kPa]	$u(Q)_p$[m^3/s]	$u(P_{el})_p$[W]	$u(m)_p$[m]	$u(\gamma)_p$[N/m^3]	$u(\eta_{el})_p$
0,00	0,41	0,000039	5,8	0,0	8,46	0,000
$u(p_e)$[kPa]	**$u(p_s)$[kPa]**	**u(Q)[m^3/s]**	**$u(P_{el})$[W]**	**u(m)[m]**	**u(γ)[N/m^3]**	**$u(\eta_{el})$**
1,13	1,21	0,000044	12,9	0,002	8,46	0,012
		η_b=0,2883	**$u(\eta_b)$=0,007472**			

The determination of the efficiency and uncertainty of the electric motor's efficiency is based on data from the manufacturer's table. For an operation point (power), the corresponding value of efficiency is taken at the table. The motor's efficiency is considered constant in this point, in other words, $u(\eta_{el})_{process}$ null. The manufacturer's table presents three efficiency values corresponding to three points of operation, defined in power percentage of 50%, 75% and 100% of the motor's nominal power, which corresponds to the electric efficiency of 79%, 82% and 83% respectively. In overload operation, the motor's efficiency remains constant (Marques et all, 2001). Thus, the uncertainty due to the meter (table) in points of overload is null. In other points (refer to table 4), the rectangular distribution for the estimation of $u(\eta_{el})_{meter}$ is considered, according to the following:

$$u(\eta_{el}) = \sqrt{u(\eta_{el})_{meter}^{\ 2} + u(\eta_{el})_{process}^{\ 2}} = u(\eta_{el})_{meter}$$

$$\overline{\eta}_{el} = \frac{0{,}79 + 0{,}83}{2} = 0{,}81$$

$$Emáx = 0{,}83 - 0{,}81 = 0{,}02$$

$$u(\eta_{el})_{meter} = \frac{E_{máx}}{\sqrt{3}} = \frac{0{,}02}{\sqrt{3}} = 0{,}012$$

The expanded uncertainty $U(\eta_b)$ is determined from the combined uncertainty (Eqs. 9a and 9b), of the number of effective levels of freedom and the corresponding Student's coefficient. The number of effective levels of freedom shall be determined with the aid of Welch - Satterthwaite equation (Eq. 16)

$$\frac{u(\eta_b)^4}{\nu_{\eta_b}} = \frac{u^*(p_e)^4}{\nu_{p_e}} + \frac{u^*(p_s)^4}{\nu_{p_s}} + \frac{u^*(m)^4}{\nu_m} + \frac{u^*(\gamma)^4}{\nu_\gamma} + \frac{u^*(Q)^4}{\nu_Q} + \frac{u^*(P_{el})^4}{\nu_{P_{el}}} + \frac{u^*(\eta_{el})^4}{\nu_{\eta_{el}}} \qquad (16)$$

The level of freedom ν_x of the variables obtained by direct measurement with the aid of (17) is determined, where $\nu_{x\ meter} \approx \infty$, e $\nu_{x\ process}$ is equal to n less 1, using variables of the type $u^*(x)_{meter}$ and $u^*(x)_{process}$.

$$\frac{u^*(x)^4}{\nu_x} = \frac{\left(u^*(x)_{meter}\right)^4}{\nu_{x\,meter}} + \frac{\left(u^*(x)_{process}\right)^4}{\nu_{x_{process}}} \qquad (17)$$

Taking point 4 as example, there is (refer to Eq. 9a and Table 3):

$$u(\eta)=\sqrt{\left(3{,}8x10^{-3}\right)^2+\left(4{,}1x10^{-3}\right)^2+\left(4{,}7x10^{-5}\right)^2+\left(9{,}0x10^{-6}\right)^2+\left(2{,}207x10^{-3}\right)^2+\left(1{,}787x10^{-3}\right)^2+\left(4{,}1x10^{-3}\right)^2}=0{,}00747$$

$$u^*(p_s)=\frac{5{,}773x10^{-3}\,m^3/s}{0{,}82x2081{,}9W}1{,}21x10^3\,Pa=0{,}00406$$

$$u^*(p_s)meter=\frac{5{,}773x10^{-3}m^3/s}{0{,}82x2081{,}9W}1{,}13\,kPa=0{,}00382$$

$$u^*(p_s)process=\frac{5{,}773x10^{-3}m^3/s}{0{,}82x2081{,}9W}0{,}41\,kPa=0{,}00139$$

$$\frac{(4{,}06x10^{-3})^4}{\nu_{ps}}=\frac{\left(3{,}82x10^{-3}\right)^4}{\infty}+\frac{\left(1{,}39x10^{-3}\right)^4}{9}$$

Table 3: Levels of freedom of the variables (operation point nº 4). The m and p indexes mean measuring device and process, respectively.

p_e[kPa]	p_s[kPa]	$Qx10^3$[m^3/s]	P_{el}[W]				
$u(p_e)$[kPa]	$u(p_s)$[kPa]	$u(Q)$[m^3/s]	$u(P_{el})$[W]	u(m)[m]	$u(\gamma)$[N/m^3]		
1,13	1,21	0,000044	12,9	0,002	8,46		
$u^*(p_e)$	**$u^*(p_s)$**	**$u^*(Q)$**	**$u^*(P_{el})$**	**u^* (m)**	**$u^*(\gamma)$**	**$u^*(\eta_{el})$**	$u(\eta_b)$
$3{,}8x10^{-3}$	$4{,}1x10^{-3}$	$2{,}21x10^{-3}$	$1{,}78x10^{-3}$	$4{,}7x10^{-5}$	$9{,}01x10^{-6}$	$4{,}1x10^{-3}$	$7{,}4x10^{-3}$
$u^*(p_e)_m$	$u^*(p_s)_m$	$u^*(Q)_m$	$u^*(P_{el})_m$	$u^*(m)_m$	$u^*(\gamma)_m$		
$3{,}83x10^{-3}$	$3{,}82x10^{-3}$	$9{,}99x10^{-4}$	$1{,}60x10^{-3}$	$5{,}7x10^{-5}$	0,0		
$u^*(p_e)_p$	$u^*(p_s)_p$	$u^*(Q)_p$	$u^*(P_{el})_p$	$u^*(m)_p$	$u^*(\gamma)_p$		
$3{,}16x10^{-18}$	$1{,}38x10^{-3}$	$1{,}96x10^{-3}$	$7{,}98x10^{-4}$	0,0	$9{,}01x10^{-6}$		
ν_{pe}	ν_{ps}	ν_Q	ν_{Pel}	ν_m	ν_γ	$\nu_{\eta el}$	$\nu_{\eta b}$
∞	655	14	227	∞	9	∞	1460

$u^+(p_e)$[m]	**$u^+(p_s)$[m]**		**u^+(m)[m]**	**$u^+(\gamma)$[m]**		
0,12	0,12		0,002	0,007		

		$u^\circ(P_{el})$[W]		**$u^\circ(\eta_{el})$[W]**
		10,58		24,04

After the effective level of freedom is known $\nu_{\eta b}$, as 1,460, there is the t Student's coefficient 1.962 in table and the efficiency of the pump at the considered point.

$$\eta_b=0{,}2883\pm1{,}962x0{,}0074=0{,}2883\pm0{,}0146$$

$$\eta_b=28{,}83\%\pm1{,}46\%$$

Similarly, with the aid of equations 10 and 10b and using the presented methodology, the manometric height is obtained. For the operation point there is:

$$H = 8{,}71m \pm 0{,}33m$$

Similarly, with the aid of equations 11 and 11b and using the presented methodology, the axis power is obtained. For the operation point there is:

$$P_{axis} = 2081{,}9W \pm 53{,}1W$$

6 RESULTS

The results of tests are presented in table 4 and in the characteristic curves of the pump in Figures 7, 8 and 9.

Table 4: Tests results

Point	Q	u(Q)x10^3	H	U(H)	Pel	u(P_{el})	P_{axis}	U(P_{axis})	η_{el}	u(η_{el})	η_b	U(η_b)
	[m^3/h]	±[m^3/s]	[m]	±[m]	[W]	±[W]	[W]	±[W]	[%]	±[%]	[%]	±[%]
1	0,0	0,0	8,63	0,32	1392,0	13,3	1141,4	38,1	82	0.012	0,0	0,0
2	5,0	0,015	8,64	0,62	1563,5	16,2	1282,1	44,2	82	0,012	9,2	0,6
3	10,0	0,021	8,73	0,33	1730,7	12,0	1419,1	43,6	82	0,012	16,7	0,8
4	20,8	0,044	8,71	0,33	2081,9	12,9	1707,2	51,5	82	0,012	28,8	1,5
5	30,5	0,052	8,53	0,33	2288,3	13,0	1899,3	21,2	83	0,0	37,3	1,5
6	39,9	0,064	8,37	0,33	2528,2	12,0	2098,4	19,6	83	0,0	43,3	1,9
7	50,6	0,098	8,08	0,46	2835,9	12,2	2353,7	19,8	83	0,0	47,2	2,2
8	60,5	0,146	7,59	0,34	3052,4	14,6	2533,5	24,2	83	0,0	49,2	2,4
9	63,6	0,118	7,47	0,34	3127,8	15,3	2596,1	25,60	83	0,0	49,8	2,4

Results obtained with the eq. 9a show variables p_e, p_s and Q as the higher sources uncertainty on the efficiency determination η_b (refer to type u* variables, Table 3). The variable η_{el} has significant interference on the uncertainty of η_b only in the 4 first points of operation. For these points, the power and efficiency values of the electric motor are not contained in the manufacturer's table, constituting a source of important uncertainty on the determination of η_b.

In the measurement of p_s, the uncertainty relative to the measuring device's characteristics is higher than the uncertainty related to the process being studied (refer to $u(p_s)_m$ and $u(p_s)_p$, table 2) . The same is verified to p_e. At the measurement of Q, the uncertainty relative to the measuring device's characteristics is lower than the uncertainty related to the process. The influence of γ and m is insignificant.

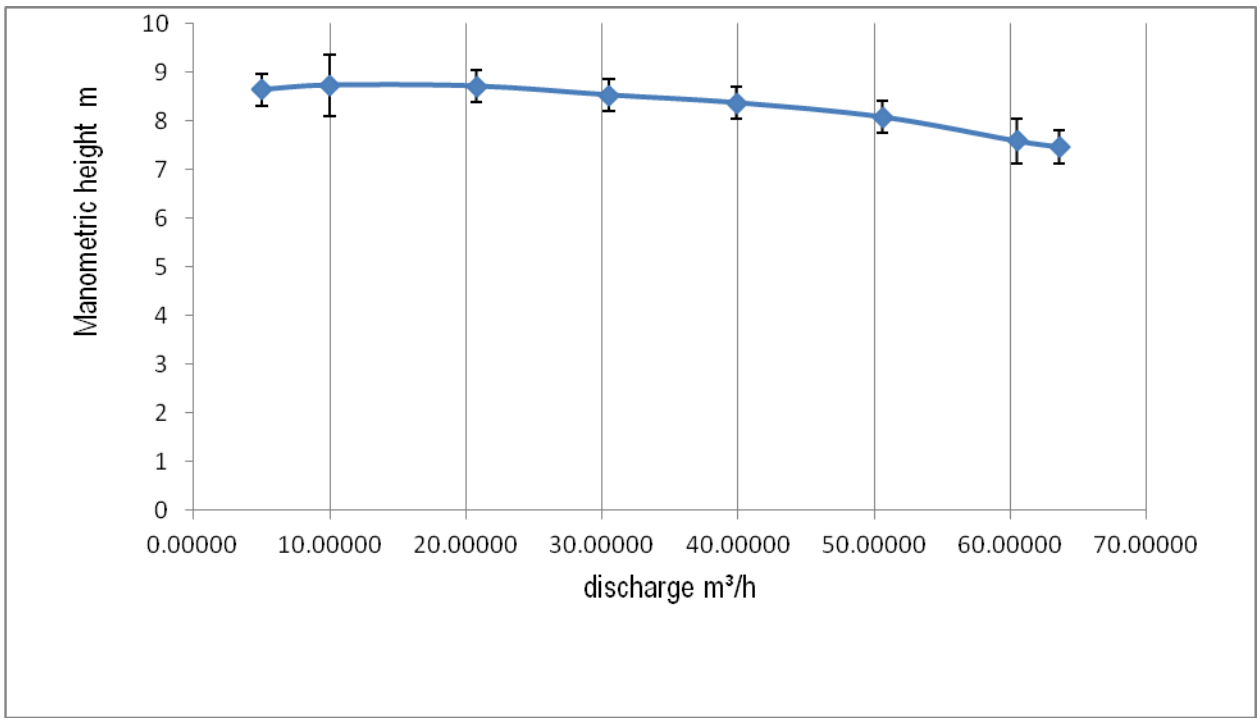

Fig. 7 – Characteristic curve of manometric height versus discharge

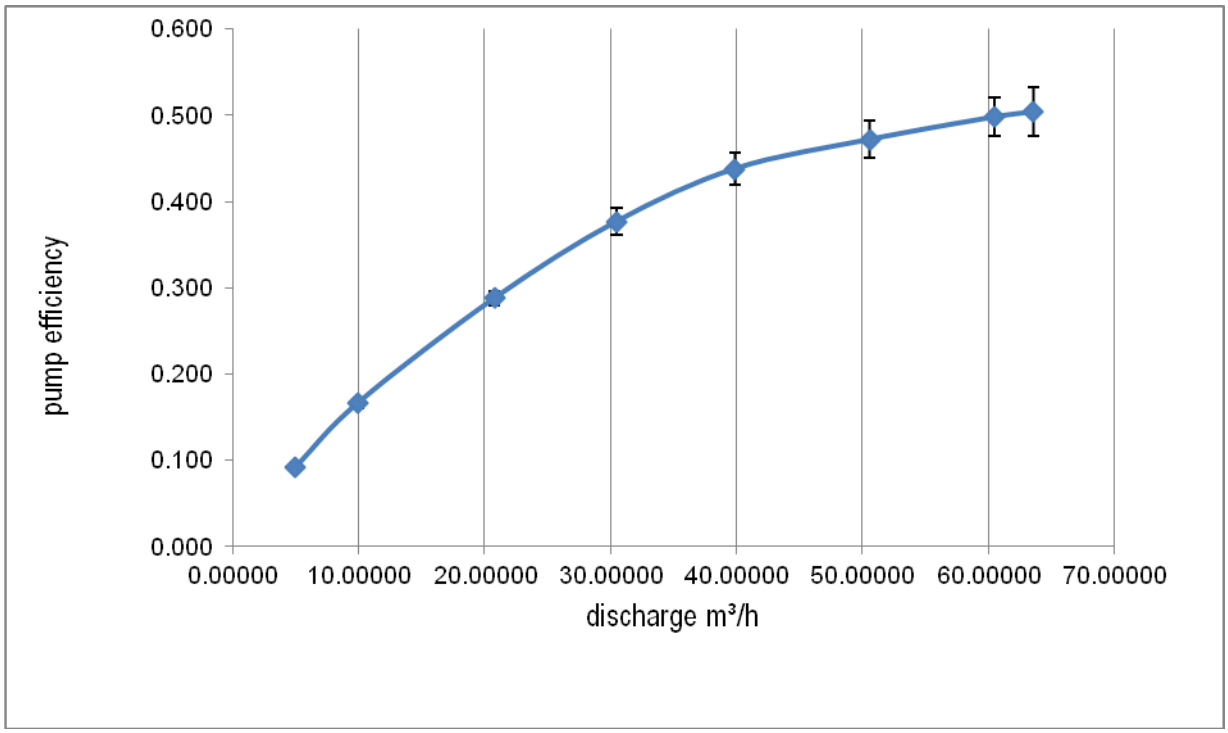

Fig. 8 – Characteristic curve of efficiency versus discharge

On the determination of the manometric height, the variables p_e and p_s constitute a higher source of uncertainty (refer to variables type u^+ at eq. 8b and table 3). The other ones can be considered as insignificant. The influence of the variables P_{el} and η_{el} (variables type u° on eq, 8c and table 3) are from the same order of magnitude.

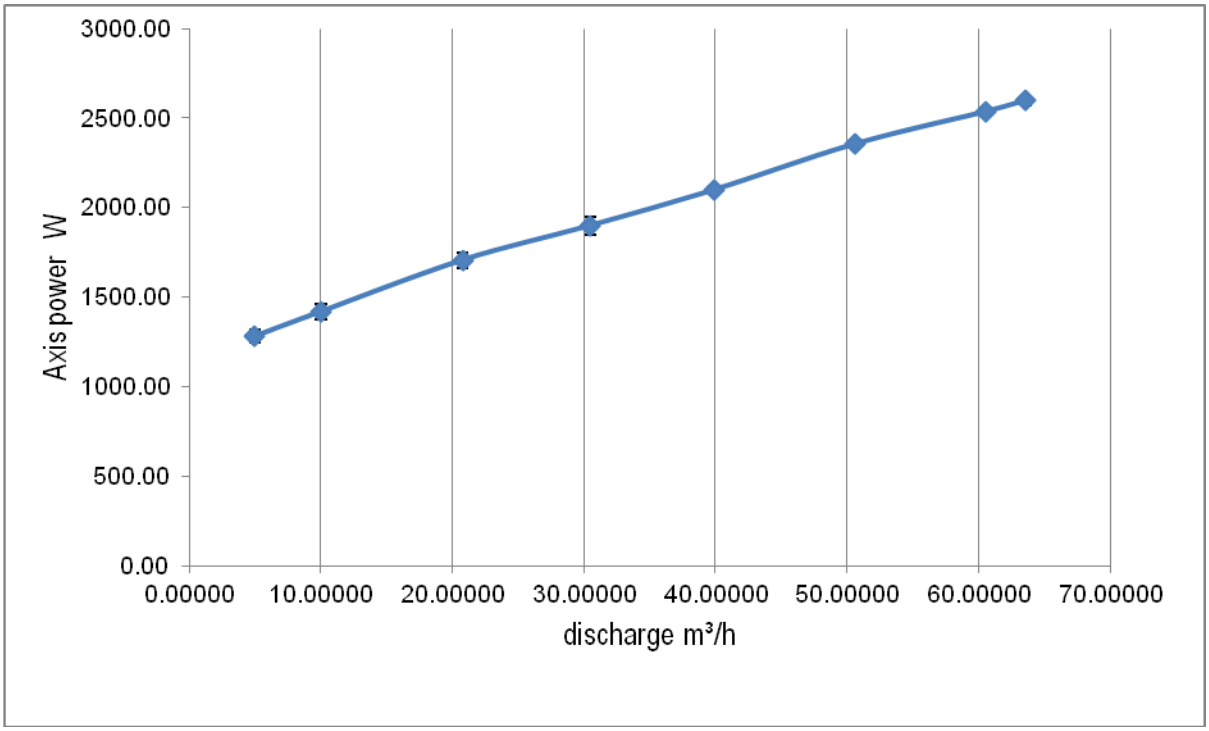

Fig. 9 – characteristic curve of axis power versus discharge

7 CONCLUSIONS

The main objective of the research was reached with the building of the characteristic curves of UFMG / CPH pump as base result and expanded uncertainty. Knowing the magnitude of the results uncertainty is in a precious information, since it makes possible a reliable analysis and consequently, reaching conclusions. The performance curves obtained are very interesting, also because, without a better understanding, there is no serial production of similar equipment which could be taken as reference.

When determining the pump's efficiency, the variable with largest influence is the pressure p_s at the pump's exit. The uncertainty related to the measuring device is two times over the uncertainty of the process. The replacement of the measuring device, related to the process' uncertainty would make possible results of better quality.

The electric motor's efficiency is a variable that, in part of the pump's operation range would cause the influence of the same order of magnitude of the pressure gauge. The availability of a motor's efficiency curve could lead to lower uncertainty of the results.

The uncertainty of the flow meter is half or less than half the uncertainty of the process. There is no influence of the measuring device on the result. The influence of the quota between pressure gages and the temperature is insignificant. The uncertainty of the electric power meter is the same or higher than the uncertainty of the process, however, its influence on the pump's income determination is also lower than the flow influence.

REFERENCES

1. Oliveira, J. E. T., 2010, http://www.oabsp.org.br/comissoes2010/defesa-consumidor/artigos/energia_eletrica.pdf/download, consulted on 15/07/2014.

2. Almeida Júnior, A. & Hernandez, F.B.T.,2001, http://www.agr.feis.unesp.br/avp280601.htm, consulted on15/07/2014.

3. Mora, D, Iglesias, P, Martinez, F, Fuertes, V., 2012. Diseño de redes de distribución de água utilizando algoritmos SFL, SEREA 2012, July 2 to 4, Coimbra.

4 Andrade, G. L., 1967. Máquinas Operatrizes Hidráulicas Escola de Engenharia da UFMG. Belo Horizonte.

5. Salcedo, C, Páez, D, Hernandez, D, Manrique L, Saldarriaga, J, 2013. "Diseño optimizado de redes abiertas com demandas dependientes de La pression usando programa lineal", XII Simposio Iberoamericano sobre planificacion de sistemas de abastecimiento y drenage, Buenos Aires.

6. Makino D, Ribeiro L C L J, Luvizzoto E, Hidalgo I G, Andrade, J G P, 2012. Eficiência energética em sistemas de abastecimento de água usando bombas de rotação variável, SEREA 2012, July 2 to 4, Coimbra.

7. Camboim, W L L, Silva, S A, Gomes H P, Souza R, Carvalho P S O, 2012. Operação de sistemas de abastecimento de água, com conjuntos motor bomba associados em paralelo, acionados com conversor de freqüência, SEREA 2012, July 2 to 4, Coimbra.

8. Valentim, C E, 2008. Otimização do desempenho de rotores de bombas hidráulicas de fluxo a partir de critérios clássicos de projeto – verificações experimentais, São Paulo, Master's Thesis of Escola Politecnica da Universidade de São Paulo.

9. Nascimento Filho et al, 2009. Caracterização de uma bancada didática de ensaios de turbobombas: um estudo metrológico, COBENGE, Recife.

10. Nascimento Filho et al, 2011. Determinação experimental da eficiência de conjuntos moto bombas: diagnóstico da instrumentação, XIX Simpósio Brasileiro de Recursos hídricos, Maceió.

11. Macityre, A J, Bombas e Instalações de Bombeamento, 1983, Editora Guanabara 2, Rio de Janeiro.

12. Nascimento, J F, Castro E C J, Amaral D, Gonzalez M L y, Martinez C, 2012. Projeto e manufatura de turbobomba como alternativa de atendimento de necessidades especiais em sistemas hidráulicos, SEREA 2012, July 2 to 4, Coimbra.

13. Marques, M., Hadad, J., Martins, A.R.S. et all. 2001, Conservação de Energia, Eletrobras / Procel, Escola Federal de Engenharia de Itajubá, Brasil.